Spin-polarized scanning tunnelling microscopy: the sensitivity of the spin-dependent current asymmetry to the barrier shape

1994 J. Phys.: Condens. Matter 6 1847

(http://iopscience.iop.org/0953-8984/6/10/004)

J. Phys.: Condens. Matter 6 (1994) 1847–1856. Printed in the UK

Spin-polarized scanning tunnelling microscopy: the sensitivity of the spin-dependent current asymmetry to the barrier shape

H J Reittu

Wihuri Physical Laboratory, University of Turku, 20500 Turku, Finland

Received 11 October 1993, in final form 12 January 1994

Abstract. The influence of the barrier shape on tunnelling of spin-polarized electrons through a vacuum gap between the tip of a scanning tunnelling microscope and a magnetic sample is analysed. It is shown that the spin-dependent transmission probability of the electrons depends strongly on the form of the barrier at the sample surface. This suggests that for a detailed interpretation of the images obtained by a spin-polarized scanning tunnelling microscope the barrier shape should be known.

1. Introduction

The invention of the scanning tunnelling microscope (STM) [1] has allowed studies of surface atomic structures. This technique has potential to become a powerful tool also for investigations into surface magnetism [2–6]. It is hoped that STMs with spin-resolving properties (SP STMs) can be realized by using an STM tip as the source of spin-polarized electrons. A solution to this problem may be a tip made out of a ferro- or antiferromagnetic material [3, 4].

Recently, spin-dependent tunnelling of electrons between an optically pumped semiconducting (e.g. GaAs) tip and a ferromagnetic sample has been analysed [6]. The results show a significant spin asymmetry of the spin-polarized current, depending on the angle between the spin orientation of the photoelectrons and the local magnetic moment on the sample surface. However, it was found that this asymmetry depends strongly on the barrier height, U, even reversing its sign in the region of $U \leqslant 1.75$ eV.

In the theoretical investigation mentioned above [6] the tunnelling barrier was assumed to be rectangular in shape. The rectangular tunnelling potential has also been used in calculations of the flow of spin-polarized electrons through junctions between two ferromagnets [7] or between a ferro- and an antiferromagnet [3]. This can hardly be a realistic choice and therefore the problem should be analysed by using a barrier that is smooth on the atomic scale.

In this paper we will discuss the influence of the barrier shape on the spin-polarized current between an optically pumped semiconducting tip of an STM and a ferromagnetic sample.

2. Transmission probability for a smooth potential barrier

The spin-polarized electrons are created in the conduction band (c band) of the semiconducting tip by illumination with circularly polarized light. Following [6] we write the wavefunction ($\Psi_\sigma(x)$ of these electrons as

$$\Psi_\sigma(x) = C_\sigma e^{ig\cdot x} \tag{1}$$

where g is the wavevector and C_σ are the amplitudes of the spin projections $\frac{1}{2}(\sigma = \uparrow)$ or $-\frac{1}{2}(\sigma = \downarrow)$, on the direction of the quantization axis. The spin polarization of the photoelectrons can be described by the spin-density matrix ρ with the components $\rho_{\alpha\beta} = C_\alpha C_\beta^*$. It can be parametrized as

$$\rho = \tfrac{1}{2}(\mathbf{I} + \boldsymbol{P}\cdot\boldsymbol{\sigma}) \tag{2}$$

where $\mathbf{I}$ is the unit 2×2 matrix, $\sigma_{x,y,z}$ are the Pauli matrices and $\boldsymbol{P}$ is the spin-polarization vector. Corresponding to optical pumping with polarized light $\boldsymbol{P}$ can be expressed as

$$\boldsymbol{P} = -\boldsymbol{n}P_0\sin(\xi) \tag{3}$$

where P_0 is a parameter ($0 \leqslant P_0 \leqslant 1$) that defines the maximum degree of the polarization ($P = |\boldsymbol{P}|$) and $\sin(\xi)$ is determined by the polarization state, being 1 (-1) for right-(left-) hand circularly polarized light. The unit vector $\boldsymbol{n}$ points along the direction of the light propagation.

In the ferromagnetic sample we assume nearly free electron states

$$\Psi_\sigma \propto e^{ik_\sigma\cdot x} \qquad \sigma = \uparrow, \downarrow\,. \tag{4}$$

From here on the spin states 'up' $\uparrow$ ('down' $\downarrow$) define the majority (minority) spin in the ferromagnet. The symbols $k_\uparrow$ and $k_\downarrow$ represent the electron momenta at the Fermi level. For instance in Fe they are ~ 1.09 Å^{-1} and ~ 0.42 Å^{-1}, respectively [8].

Let us now consider tunnelling of electrons through the barrier potential $U(x)$ shown in figure 1. We suppose that the bias voltage is adjusted so that the bottom of the semiconductor c band is at the Fermi level of a ferromagnetic sample located in the region $x > d$. The semiconducting tip is located at $x < -d$. The shape of the potential $U(x)$ can be adjusted by a parameter a so that it approaches a rectangular barrier at the limit $a = 0$. Physically 'a' can be understood as the thickness of an electric dipole layer located on the surface of the sample and on that of the tip [9]. To allow the calculations to be made analytically we take the potential in the form [10]

$$U(x) = \begin{cases} U_r(x) = (U + U_0 + \boldsymbol{H}\cdot\boldsymbol{\sigma})/(1 + e^{(x-d)/a}) - U_0 - \boldsymbol{H}\cdot\boldsymbol{\sigma} & x > 0 \\ U_l(x) = U/(1 + e^{-(x+d)/a}) & x \leqslant 0 \end{cases} \tag{5}$$

where $2d$ is the width of the barrier and $\boldsymbol{H}$ is the exchange field inside the ferromagnet. $\boldsymbol{H}$ defines the direction of the quantization axis (z-axis). Thus we can write $\boldsymbol{H}\cdot\boldsymbol{\sigma} = H\sigma_z$ with $H = |\boldsymbol{H}|$. In the bulk of the ferromagnet we have $U_r = -U_0 - H\sigma_z$. Within the surface layer of thickness $\sim a$ the magnitude of the spin-dependent part of $U(x)$ decreases smoothly to zero. The meanings of the parameters U and U_0 can be seen from figure 1.

For the sake of simplicity we consider here the 1D problem. As will be seen later this is not a principal restriction in our case. It is also supposed that the electron effective mass of the semiconductor c electrons is equal to the free electron mass m_e. This assumption can be used because we are interested in the value of the spin asymmetry, A, of the tunnelling current. As will be seen A is insensitive to the value of the effective mass of the electrons.

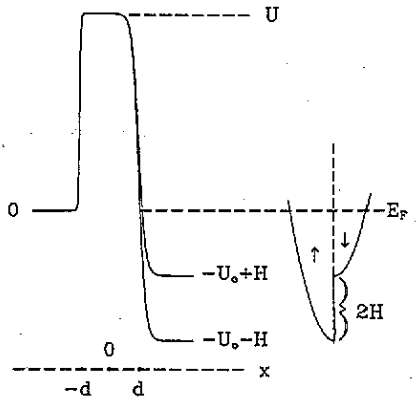

Figure 1. A schematic representation of the potential barrier between the tip ($x < -d$) and the sample ($x > d$). E_F is the Fermi level of the ferromagnet. The zero potential is taken at the bottom of the c band of the tip. The energy U denotes the vacuum level; $-U_0 \pm H$ is the potential energy at the bottom of the c band of the ferromagnet. The electron bands in the ferromagnet are represented by two halves of a parabola. With energy $\leqslant E_F$ they are occupied by electrons with the majority (↑) or minority (↓) spins.

We treat a barrier wide enough that the tunnelling rate is low. Then it is possible to use Bardeen's perturbation method [11] to find the transmission probability per unit time for an electron with spin component σ,

$$w_\sigma = (2\pi/\hbar)|M_\sigma|^2 \rho_\sigma(E). \tag{6}$$

Here $\rho_\sigma(E)$ is the density of the electron states in the ferromagnet. In the 1D case ρ_σ takes the form [12]

$$\rho_\sigma = m_e/\pi\hbar^2 k_\sigma \tag{7}$$

The transition matrix element M_σ can be given as

$$M_\sigma = -(\hbar^2/2m_e)(\Psi^*_{r\sigma}\, d\Psi_{l\sigma}/dx - \Psi_{l\sigma}\, d\Psi^*_{r\sigma}/dx) \tag{8}$$

where $\Psi_{r\sigma}$ and $\Psi_{l\sigma}$ are the wavefunctions of the electrons at the energy $E < U$ within the potentials $U_r(x)$ and $U_l(x)$ respectively. The wavefunctions and their derivatives appearing in (8) are defined at any point inside the barrier (e.g. $x = 0$).

3. Tunnelling current asymmetry

The wavefunction $\Psi_{l\sigma}$ is the eigenfunction ($E < U$) of the Schrödinger equation with the Hamiltonian

$$H_l = p^2/2m_e + U_l(x) \tag{9}$$

where $p = -i\hbar d/dx$. The asymptotic behaviour of $\psi_{l\sigma}$ requires that $\Psi_{l\sigma} \to 0$ when $x \to \infty$. Similarly the wavefunction $\Psi_{r\sigma}$ is the eigenfunction ($E < U$) of the Schrödinger equation with the Hamiltonian

$$H_r = p^2/2m' + U_r(x) \tag{10}$$

where $m' \simeq m_e$ is the effective mass (m_e is the free electron mass). At the limit $x \to -\infty$, $\Psi_{r\sigma}$ must vanish.

To find $\Psi_{l\sigma}$ we solve the equation

$$(-(\hbar^2/2m_e)\,d^2/dx^2 + U/[1+\exp(-(x+d)/a)])\Psi_{l\sigma} = E\Psi_{l\sigma}. \tag{11}$$

The result is (see the appendix)

$$\Psi_{l\sigma}(x) = L_\sigma e^{-\kappa(x+d)} F(\kappa a + ika, \kappa a - ika; 1 + 2\kappa a; z_l) \tag{12}$$

where L_σ, κ, $F(\kappa a + ika, \kappa a - ika; 1 + 2\kappa a; z_l)$, k and z_l are given in the appendix by (A13), (A3), (A8) and (A1).

Now $\Psi_{r\sigma}$ is found from the Schrödinger equation with the Hamiltonian defined by (10) and (5). The result is (see the appendix)

$$\Psi_{r\sigma} = N_\sigma e^{\kappa(x-d)} F(\kappa a + ik_\sigma a, \kappa a - ik_\sigma a; 1 + 2\kappa a; z_r) \tag{13}$$

where N_σ, k_σ and z_r are given by (A18) and (A19).

The transmission probability w_σ can be calculated from (6–8). We take the values of the wavefunctions and their derivatives in (8) at the point $x = 0$ and assume that the tunnelling gap is wide in comparison with the value of the parameter a. Then we have $z_r(x=0) = z_l(x=0) = \exp(-d/a) \simeq 0$. At this limit (8) can be written with the help of (12) and (13) in the form

$$M_\sigma = (\hbar^2/2m_e)\kappa N_\sigma^* L_\sigma e^{-2\kappa d}. \tag{14}$$

Using (6), (7) and (14) we finally obtain

$$w_\sigma = (2\hbar\kappa^2|N_\sigma|^2|L_\sigma|^2/m_e k_\sigma)e^{-4\kappa d}. \tag{15}$$

The total tunnelling current is defined as

$$J = (w_\uparrow + w_\downarrow)e \tag{16}$$

where e is the electron charge. According to (2) and (14) we have

$$|L_\sigma|^2 = \rho_{\sigma\sigma}|L_0|^2 \tag{17}$$

with

$$\begin{cases} \rho_{\uparrow,\uparrow} = \frac{1}{2}(1 - P_0\cos(\theta)\sin(\xi)) \\ \rho_{\downarrow,\downarrow} = \frac{1}{2}(1 + P_0\cos(\theta)\sin(\xi)). \end{cases} \tag{18}$$

Here θ is the angle between the quantization axis (parallel to $\boldsymbol{H}$) and the direction of the light propagation (along $\boldsymbol{n}$). With (15)–(18) the total current is

$$J = J_\uparrow + J_\downarrow + (J_\downarrow - J_\uparrow)P_0\cos(\theta)\sin(\xi) \tag{19}$$

with

$$J_\sigma = (\hbar e\kappa^2|N_\sigma|^2|L_0|^2/m_e k_\sigma)e^{-4\kappa d}. \tag{20}$$

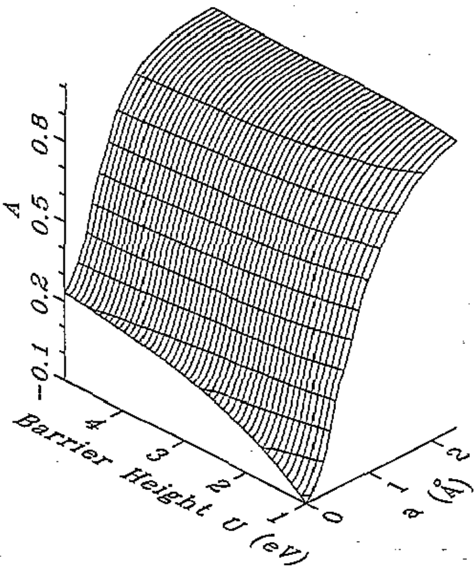

Figure 2. The spin-dependent current asymmetry A for different values of the barrier height (U) and the thickness (a) of the electric dipole layer at the surfaces of the tip and the sample. The result for a rectangular barrier is given by the intersection line between the surface $A = A(U, a)$ and the plane $a = 0$.

The asymmetry between currents of the electrons with opposite spins can be defined as

$$A = (J_\uparrow - J_\downarrow)/(J_\uparrow + J_\downarrow). \tag{21}$$

By using (A13), (A18), (20) and (21) we can write

$$A = (A_\uparrow - A_\downarrow)/(A_\uparrow + A_\downarrow) \qquad A_\sigma = (\kappa^2 + k_\sigma^2)\sinh(2\pi k_\sigma a)|\Gamma^2(\kappa a - \mathrm{i}k_\sigma a)|^2. \tag{22}$$

To derive (22) we employed the well known formula $|\Gamma(\mathrm{i}y)|^2 = \pi/(y\sinh(\pi y))$, with real y. The dependences of A on the parameter a and the barrier height $U \propto \kappa^2$ are shown in figures 2 and 3.

It was assumed above that the electron effective mass $m^* = m_e$. However, inside the semiconducting tip $m^* \ll m_e$ (e.g. in the case of GaAs $\simeq 0.07m_e$). Let us define the correct form of (22) with the realistic value of m^* inside the semiconducting tip. The change of m^* at the tip–vacuum boundary would have the effect of modifying the wavefunction $\Psi_{l\sigma}$. These changes are obviously (see the appendix) absorbed in the coefficient L_0 and since this is spin independent they do not affect the value of A. We can see therefore that (22) is valid also in the case $m^* \ll m_e$.

We may also neglect the dependence of A on the kinetic energy of the photoelectrons through κ and k_σ given by (A3) and (A19), respectively. This energy ($\hbar^2k^2/2m^*$) is typically of the order of 10^{-2} eV [13] and is defined by the effective photoelectron temperature. In the case of GaAs this leads to a value of $k \simeq 10^{-2}$ Å^{-1}. Since the magnitudes of $\kappa(k = 0)$ and $k_\sigma(k = 0)$ are of the order of 1–0.1 Å^{-1} we may take the values of κ and k_σ at $k = 0$ (the errors induced in the value of A do not exceed 1%). This justifies also the 1D approximation used to derive (22) because it is not necessary to consider k as a 3D vector quantity since we are totally ignoring the dependence of A on k.

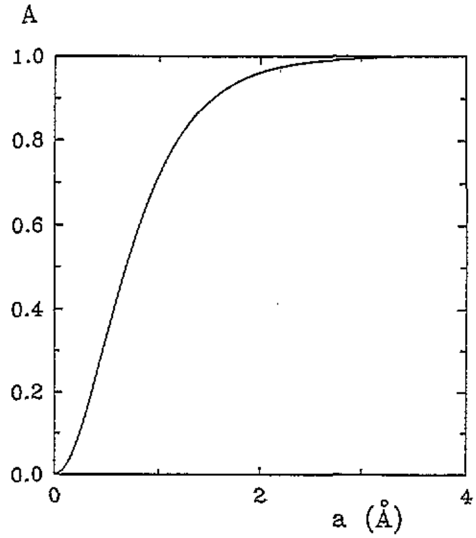

Figure 3. The dependence of the spin-polarized current asymmetry on the parameter a at the barrier height $U = 1.75$ eV. This dependence is parabolic at small values (< 0.1 Å) of a. When a is increased A approaches unit value exponentially.

Using the approximations $\Gamma(\varepsilon) \simeq 1/\varepsilon$ and $\mathrm{sh}(\varepsilon) \simeq \varepsilon$ for $|\varepsilon| \ll 1$, we may write at the limit $a \to 0$

$$A = (k_\uparrow - k_\downarrow)(\kappa^2 - k_\uparrow k_\downarrow)/(k_\uparrow + k_\downarrow)(\kappa^2 + k_\uparrow k_\downarrow). \tag{23}$$

This expression coincides with the result obtained earlier by using a rectangular barrier shape [6].

When a is large enough A approaches exponentially a plateau corresponding to $A = 1$. This can be verified by substituting for the gamma function $\Gamma(\kappa a - \mathrm{i}k_\sigma a)$ its asymptotic form

$$\Gamma(z) \simeq z^{z-1/2}\mathrm{e}^{-z}\sqrt{2}\pi \qquad |z| \gg 1.$$

As a result the current asymmetry can be written as

$$A \simeq 1 - 2\exp[-2\kappa a(\Phi_\uparrow - \Phi_\downarrow)] \tag{24}$$

with

$$\Phi_\sigma = \ln(1 + k_\sigma^2/\kappa^2) + (k_\sigma/\kappa)(\pi - 2\tan^{-1}(k_\sigma/\kappa)). \tag{25}$$

Here Φ_σ is a monotonically growing function of k_σ/κ, indicating that $\Phi_\uparrow > \Phi_\downarrow$ since $k_\uparrow > k_\downarrow$.

4. Discussion and conclusions

The dependence of the tunnelling current asymmetry on the parameters κ and a (see (22)) is shown in figure 2. It can be seen that the result is highly dependent on the value of a on the scale of a few ångströms. For values of $a \geqslant 1$ Å the asymmetry A increases to nearly unity and has no zero point as in the case of the rectangular barrier [6]. When a is increased A approaches a plateau (see (24) and (25)). Between the values of $a = 0$ and 2 Å the increase of A is very steep.

From (22) and (23) we can see the limits of the validity of the assumption about the rectangular barrier. By expanding (22) with respect to a, it is found that the first correction term is quadratic in a. The quadratic terms are $(a\kappa)^2$, $a^2\kappa k_\sigma$ and $(ak_\sigma)^2$. The values of κ and k_σ are typically of the order of 1 $Å^{-1}$. Therefore corrections to the rectangular barrier model are insignificant ($< 1\%$) only when $a \lesssim 10^{-1}$ Å. This is supported also by figures 2 and 3. According to the theory of Lang and Kohn [14] the thickness (a) of the dipole layer at the surface can be several ångströms.

We expect that the results for other types of SP STMs would be similar to those in the present paper. Slonczewski remarks in [7] that the discontinuous change of the potential at the electrode barrier interface between two ferromagnets predicts a smaller spin-polarization factor than that found in experiments. This agrees qualitatively with results of the present calculation.

In our model of the SP STM [6] the signal is due to modulation of the helicity of the circularly polarized pumping light (e.g. $\sin(\xi) = \sin(\Omega t)$), causing in the tunnelling current oscillations with amplitude proportional to A ((19)–(22)). In an ideal case changes of A can be associated with magnetic properties of the sample surface (k_σ and θ). For instance within a ferromagnetic domain wall the rotation of the spins would cause alternations of the angle θ. As is evident from (19), this changes the amplitude of the oscillating current signal. As was pointed out in section 3 this amplitude can be influenced also by local modulation of the potential barrier e.g. by adatoms on the surface [9]. However, the much higher values of A obtained by using a smoothed barrier instead of a rectangular one increase the possibility for practical realization of the SP STM.

It should be noted that within the framework of Bardeen's tunnelling theory [11] employed above the magnitude of A is defined entirely by the sample surface through the potential $U_r(x)$. The surface potential of the tip, $U_l(x)$, has impact only on the value of L_0 (see (A13)). Since L_0 is spin independent it has no effect on A.

Finally we shall summarize the physical origin of the effects described in sections 2 and 3. In the bulk of the ferromagnet the value of the effective potential for electrons with the majority spin is $-U_0 - H$ and that for electrons with the minority spin is $-U_0 + H$ (see (5) and figure 1). Within the surface region of thickness $\sim a$ these two potentials are different. Accordingly the classical turning points for the electrons with majority and minority spins are displaced from each other at some distance when the potential barrier is not rectangular ($a > 0$). On the other hand, it is well known that the probability of tunnelling through a potential barrier depends strongly on the barrier shape and the energy of the tunnelling particle. Since the potential barriers for electrons with spin 'up' and spin 'down' differ in the way described above the change of the parameter a gives rise to the tunnelling current asymmetry as shown in section 3.

Acknowledgments

The author is obliged to Dr Reino Laiho for valuable contributions and a critical reading of the manuscript. The financial support of the Wihuri Foundation is gratefully acknowledged.

Appendix

We substitute a new variable

$$z_1 = -\exp(-(x+d)/a) \tag{A1}$$

in (11), transforming it to the form

$$z_1^2(1-z_1)\Psi''_{1\sigma} + z_1(1-z_1)\Psi'_{1\sigma} - (\kappa^2 + z_1 k^2)a^2\Psi_{1\sigma} = 0 \tag{A2}$$

where the prime denotes the derivation $\mathrm{d}/\mathrm{d}z_1$ and

$$\kappa = [2m_e(U-E)/\hbar^2]^{1/2} \qquad k = [2m_e E/\hbar^2]^{1/2}. \tag{A3}$$

Writing

$$\Psi_{1\sigma}(z_1) = w_{1\sigma}(z_1)(z_1)^{\kappa a} \tag{A4}$$

(A2) is transformed to

$$z_1(1-z_1)w''_{1\sigma} + (1-z_1)(1+2\kappa a)w'_{1\sigma} - [(\kappa a)^2 + (ka)^2]w_{1\sigma} = 0 \tag{A5}$$

which is actually the hypergeometric equation [15]

$$z(1-z)u''(z) + [\gamma - (\alpha+\beta+1)z]u'(z) - \alpha\beta u(z) = 0. \tag{A6}$$

The independent solutions of (A6) are

$$\begin{aligned} u_1 &= F(\alpha,\beta;\gamma;z) \\ u_2 &= z^{1-\gamma}F(\alpha-\gamma+1,\beta-\gamma+1;2-\gamma;z) \end{aligned} \tag{A7}$$

where the hypergeometric function $F(\alpha,\beta;\gamma;z)$ is defined by the following serial expansion for $|z| < 1$:

$$F(\alpha,\beta;\gamma;z) = 1 + (\alpha\beta/\gamma)z/1! + [\alpha(\alpha+1)\beta(\beta+1)/\gamma(\gamma+1)]z^2/2! + \dots. \tag{A8}$$

To continue the function $F(\alpha,\beta;\gamma;z)$ analytically to the region $|z| > 1$ and to have asymptotic expansions for $|z| \to \infty$, we use the well known transformation

$$\begin{aligned} F(\alpha,\beta;\gamma;z) = {} & \frac{\Gamma(\gamma)\Gamma(\beta-\alpha)}{\Gamma(\beta)\Gamma(\gamma-\alpha)}(-1)^{\alpha}z^{-\alpha}F(\alpha,\alpha+1-\gamma;\alpha+1-\beta;1/z) \\ & + \frac{\Gamma(\gamma)\Gamma(\alpha-\beta)}{\Gamma(\alpha)\Gamma(\gamma-\beta)}(-1)^{\beta}z^{-\beta}F(\beta,\beta+1-\gamma;\beta+1-\alpha;1/z) \end{aligned} \tag{A9}$$

where $\Gamma(x)$ is Euler's gamma function.

According to (A5) and (A6) we have

$$\alpha = \kappa a + ika \qquad \beta = \kappa a - ika \qquad \gamma = 1 + 2\kappa a. \tag{A10}$$

(A1), (A4), (A7), (A8) and (A9) indicate that the only solution of (11) with the limit $\Psi_{l\sigma} \to 0$ for $x \to \infty$ is

$$\Psi_{l\sigma}(x) = L_\sigma e^{-\kappa(x+d)} F(\alpha, \beta; \gamma; z_l). \tag{A11}$$

The coefficient L_σ is determined from the initial condition

$$\Psi_{l\sigma}(x) \to C_\sigma e^{ikx} + R_\sigma e^{-ikx} \qquad x \to -\infty. \tag{A12}$$

For $x \to -\infty$ z_l has the limit $-\infty$. That is why we can use (A9) and (A10) to obtain the asymptote of $\Psi_{l\sigma}$ as $z_l \to -\infty$. By matching this with $\Psi_{l\sigma}$ in (A12) we find

$$L_\sigma = C_\sigma L_0 \qquad L_0 = (\kappa - ik)\Gamma^2(\kappa a - ika)e^{-ikd}/2\kappa\Gamma(2\kappa a)\Gamma(-2ika). \tag{A13}$$

Finally the solution of equation (11) is obtained with (A1), (A10), (A11) and (A13) in the form

$$\Psi_{l\sigma}(x) = C_\sigma e^{-\kappa(x+d)} L_0 F(\kappa a + ika, \kappa a - ika; 1 + 2\kappa a; z_l). \tag{A14}$$

The equation for $\Psi_{r\sigma}$ is (see (5) and (10))

$$(-(\hbar^2/2m_e)\, d^2/dx^2 + U_r(x))\Psi_{r\sigma} = E\Psi_{r\sigma}. \tag{A15}$$

The initial condition can be written as (see (4))

$$\Psi_{r\sigma}(x) \to e^{-ik_\sigma x} + r_\sigma e^{ik_\sigma x} \qquad x \to \infty. \tag{A16}$$

At the limit $x \to -\infty$ $\Psi_{r\sigma}$ must vanish.

The solution of (A15), (A16) can be found in a similar way as that above to solve (11). The final result is

$$\Psi_{r\sigma} = N_\sigma e^{\kappa(x-d)} F(\kappa a + ik_\sigma a, \kappa a - ik_\sigma a; 1 + 2\kappa a; z_r) \tag{A17}$$

with

$$N_\sigma = e^{ik_\sigma d}(\kappa - ik_\sigma)\Gamma^2(\kappa a - ik_\sigma a)/2\kappa\Gamma(2\kappa a)\Gamma(-2ik_\sigma a) \tag{A18}$$

and

$$k_\sigma = [2m_e(E + U_0 \pm H)/\hbar^2]^{1/2} \qquad z_r = -\exp((x-d)/a). \tag{A19}$$

References

[1] Binnig G, Rohrer H, Gerber Ch and Weibel E 1982 *Appl. Phys. Lett.* 40 178
[2] Shvets I V, Wiesendanger R, Bürgler D, Tarrach G, Güntherodt H-J and Coey J M D 1992 *J. Appl. Phys.* 71 5489
[3] Minakov A A and Shvets I V 1990 *Surf. Sci. Lett.* 236 L377
[4] Wiesendanger R, Güntherodt H-J, Güntherodt G, Gambino R J and Ruf R 1990 *Phys. Rev. Lett.* 65 247
[5] Garcia N 1991 *Science and Technology of Nanostructured Magnetic Materials* ed G C Hajipanayis and G A Prinz (New York: Plenum) p 301
[6] Laiho R and Reittu H J 1993 *Surf. Sci.* 289 363
[7] Slonczewski J C 1989 *Phys. Rev.* B 39 6995
[8] Stearns M B 1977 *J. Magn. Magn. Mater.* 5 167
[9] Hölzl J and Schulte F K 1979 *Solid Surface Physics (Springer Tracts in Modern Physics 85)* ed G Höhler (Berlin: Springer) p 2
[10] Landau L D and Lifshitz E M 1958 *Quantum Mechanics: Non-Relativistic Theory* (Oxford: Pergamon) p 75
[11] Bardeen J 1961 *Phys. Rev. Lett.* 6 57
[12] Roy D K 1986 *Quantum Mechanical Tunneling And Its Applications* (Singapore: World Scientific) p 19
[13] Shah J and Leite R C C 1969 *Phys. Rev. Lett.* 22 1304
[14] Lang N D and Kohn W 1970 *Phys. Rev.* B 1 4555
[15] Gradshteyn I S and Ryzhik I M 1980 *Table of Integrals, Series, and Products* (New York: Academic) p 1045